Clays and Clay Minerals, Vol. 32, No. 4, 259–271, 1984.

MINERALOGY AND GENETIC RELATIONSHIPS OF TONSTEIN, BENTONITE, AND LIGNITIC STRATA IN THE EOCENE YEGUA FORMATION OF EAST-CENTRAL TEXAS

A. L. SENKAYI, J. B. DIXON, L. R. HOSSNER,
M. ABDER-RUHMAN, AND D. S. FANNING[1]

Department of Soil and Crop Sciences, Texas Agricultural Experiment Station
Texas A&M University, College Station, Texas 77843

Abstract—A kaolinite-rich bed (tonstein) and an associated bentonite in the upper part of Yegua Formation at College Station, east-central Texas, were formed by *in situ* weathering processes in a late Eocene swamp. X-ray powder diffraction, infrared spectroscopy, petrographic studies, and scanning and transmission electron microscopy not only show that dioctahedral smectite and coarsely crystalline kaolinite are the dominant minerals in the bentonite and tonstein, respectively, but that cryptocrystalline halloysite and kaolinite are localized along the weathering front (transitional zone) between the tonstein and the bentonite. As weathering progressed, the cryptocrystalline minerals gradually recrystallized to yield the coarse books and vermicular growths of kaolinite characteristic of the tonstein.

Small amounts of cristobalite, sanidine, and euhedral zircon crystals with liquid or gaseous inclusions accord with the formation of the bentonite by alteration of volcanic ash. Clinoptilolite in the lignitic layer and sandstone below the bentonite probably formed from ions that were released during alteration of the volcanic materials to smectite, but clinoptilolite in the tonstein and overlying strata appear to have formed after kaolinization of the bentonite.

Key Words—Bentonite, Clinoptilolite, Kaolinite, Lignite, Smectite, Tonstein, Weathering.

INTRODUCTION

The genesis of kaolinite-rich strata (tonsteins) in coal or lignite is still controversial (Loughnan, 1978), although it is generally believed that most tonsteins formed in swamps and basins in which significant amounts of partially decomposed organic matter were present (Millot, 1970; Williamson, 1970; Price and Duff, 1969; Spears and Kanaris-Sotiriou, 1979; Zhou *et al.*, 1982). According to this hypothesis, most tonsteins are products of the *in situ* kaolinization of volcanic ash deposited in coal-forming swamp environments. Such environments existed along the entire Gulf Coast of the United States during the Tertiary Period and resulted in the formation of extensive deposits of lignite in eastern Texas. The lignite accumulated mainly in delta plains, basins, and overbank marshes between major river channels (Kaiser, 1974). During this period, volcanic ash from sources probably in southwestern Texas, New Mexico, or northern Mexico (Roberson, 1964) was also deposited in these swamps and basins, and much of it was altered to smectite-rich beds or bentonites (Roberson, 1964).

The bentonite investigated in this study is unique because it shows an upward gradation from smectitic bentonite to kaolinitic tonstein. The gradation allows evaluation of the processes which resulted in the alteration of the bentonite to tonstein. These processes have not been fully discussed in literature. The major objectives of this study were to investigate the chemical, mineralogical and micromorphological properties of the bentonite and the associated tonstein in order to gain insight into their genetic relationships.

MATERIALS AND METHODS

Sampling

The bentonite and tonstein are exposed in gullies and banks along White Creek near Easterwood Airport, College Station, Texas (Figure 1). Three exposures (sites 1, 2, and 3) were selected for this study (Figures 1 and 2). Small sequential samples were obtained from each stratum at each of the three sites shown in Figure 2 (claystone, lignitic strata, tonstein, bentonite, and sandstone). The samples were dried at room temperature, ground, and passed through a 2.0-mm sieve. Bulk specimens were also obtained for thin sections and for examination by scanning electron microscopy.

Physical and chemical determinations

The pH (1:1 soil to water) and color of all samples were determined. Total C was determined by the LECO induction-furnace procedure (Carr, 1973). The samples were separated into sand (>50 μm), silt (50–2 μm), coarse clay (2.0–0.2 μm), and fine clay (<0.2 μm) fractions according to the procedures of Jackson (1974). Heavy liquids were employed to concentrate the heavy minerals in the silt fractions. Bulk samples from the

[1] Department of Agronomy, University of Maryland, College Park, Maryland 20742.

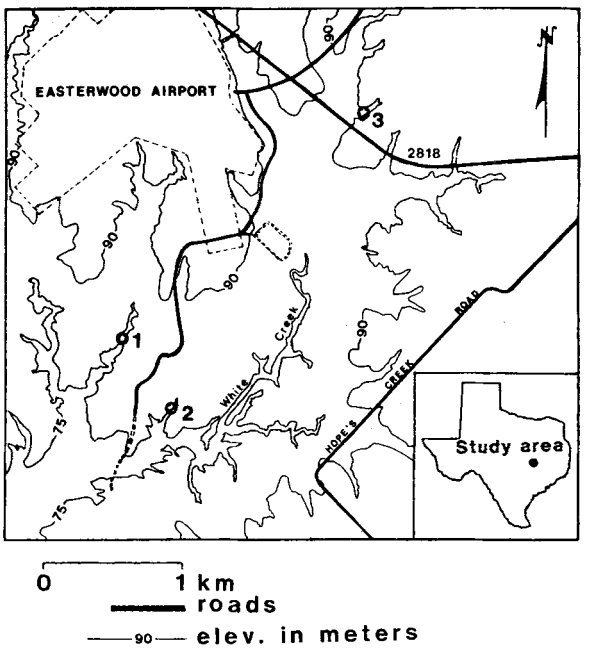

Figure 1. Map showing location of the sampling sites 1, 2, and 3 near Easterwood Airport, College Station, Texas.

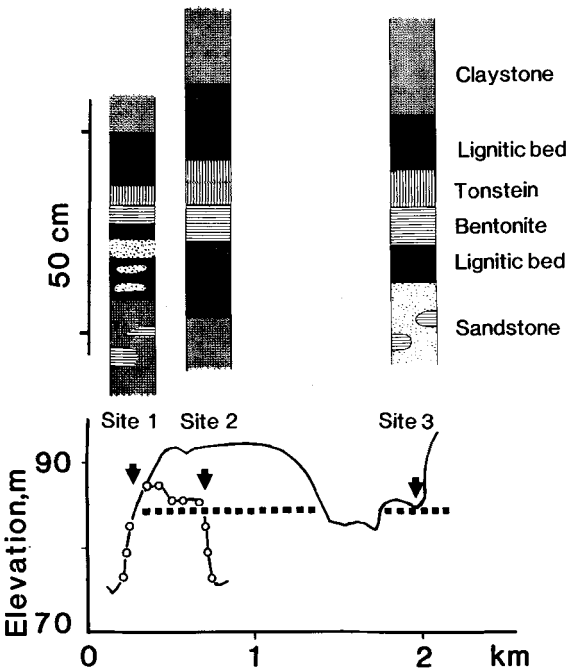

Figure 2. Cross-section (bottom part of figure) showing topographic features between sites 1 and 2 (open circles) and sites 1 and 3. The approximate stratigraphic position of the tonstein-bentonite beds (broken line) and the sequence of the major strata at the three sites (upper part of figure) are also shown.

tonsteins were also treated with HF (20% v/v HF in water) for 1 min to dissolve the kaolinite (Norrish, 1968). The remaining residue was analyzed by X-ray powder diffraction (XRD) to test for the presence of minerals of the plumbogummite series.

Optical and electron microscopy. Epoxy-impregnated thin sections were prepared according to Innes and Pluth (1970). Specimens for scanning electron microscopy (SEM) investigations were pasted on aluminum stubs, lightly coated with a thin film of sputtered-on carbon and examined with a JEOL 25II electron microscope. Transmission electron micrographs of the clay samples were obtained using a Hitachi HU-11E microscope.

X-ray powder diffraction. Whole rock and clay samples were investigated by XRD using a Philips diffractometer equipped with a graphite monochromator and Cu-target X-ray tube operated at 35 kV and 14 ma. The bulk samples were ground in acetone to a fine powder, and randomly oriented powder mounts were prepared using Al sample holders. Oriented, Mg-saturated and glycerated clay samples were also investigated by XRD.

Infrared spectroscopy. Infrared (IR) spectra of the fine (<0.2 μm) clay samples from the bentonites were obtained using a Perkin Elmer model 283 spectrophotometer and the KBr pressed-disc method.

Total elemental analysis. The finely ground bulk samples from the tonstein and bentonite strata were digested in HF overnight at room temperature. This procedure is similar to that described by Bernas (1968) except that plastic volumetric flasks were employed instead of heated digestion vessels. The major and trace elements in the resulting solutions were determined by emission spectroscopy using an inductively coupled plasma (ICP) source (Applied Research Laboratory model 3400). The operating conditions were as follows: RF generator power, 1.2 kW; nebulizer uptake, 1.6 ml/min; plasma gas, 0.8 liter/min; carrier gas, 1.0 liter/min; coolant gas 1.0 liter/min.

STRATIGRAPHY AND FIELD DESCRIPTIONS

The tonstein and bentonite strata form part of the Easterwood Shale Member of the Yegua Formation of late Eocene age in east-central Texas. The member is a distinctive local unit that also contains claystone, lignitic or carbonaceous layers, and sandstone (Mathews, 1950), for which a deltaic environment of deposition has been inferred (Berg, 1970).

At site 1, the tonstein-bentonite interval is only 10 cm thick and can be traced for about 3 m along the exposure. At sites 2 and 3, the tonstein and bentonite beds are thicker; they can be traced for about 10 m laterally at site 2 and for 30 m along the exposure at site 3. The tonstein bed is lighter in color (Table 1) and

Table 1. Properties of tonstein, bentonite, and nonvolcanic strata in the Easterwood Shale Member of Yegua Formation in east central Texas.

Strata	Depth from surface (m)	Thickness (cm)	pH	Total C (%)	Munsell color[1] (moist)	Texture[2]
Site 1						
Shale	4.0	—	6.9	0.34	Pale br (10YR6/3)	Silty clay
Lignitic shale		14.0	7.4	0.47	Dk br (7.5YR4/2)	Silty clay
Tonstein		5.1	7.2	0.61	White (10YR8/1)	Loam
Bentonite		5.0	6.9	0.32	Yellow (2.5Y7/6)	Clay
Lignitic shale		2.8	7.3	1.03	Dk red-br (5YR3/3)	Silty
Sandstone		5.1	8.0	0.00	Lt br-gr (10YR6/2)	Sand
Site 2						
Shale	1.0	20	5.5	0.23	Pale br (10YR6/3)	Silty clay
Lignitic shale		20	5.6	4.71	Dk red-br (5YR3/2)	Silty clay
Strato-tonstein		5	5.6	1.87	Reddish br (5YR5/4)	Clay
Ortho-tonstein		5	5.7	0.92	Light gr (10YR7/2)	Silty clay
Bentonite		10	5.4	0.97	Yellow (10YR7/6)	Clay
Lignitic shale		20	5.3	5.47	Black (10YR2/1)	Silty clay
Shale		14	5.3	5.47	Brown (10YR5/3)	Clay
Site 3						
Shale	1.0	20	6.0	0.00	Light br-gr (2.5Y6/2)	Clay
Lignitic shale		25	4.9	3.22	Dk red-br (5YR3/2)	Silty clay
Tonstein		10	5.9	0.22	Light gr (10YR7/2)	Silty clay
Bentonite		10	7.1	0.58	Pale gr (2.5Y7/4)	Clay
Lignitic shale		10	7.1	0.91	Dk red-br (5YR3/2)	Silty clay
Sandstone		20	6.3	0.35	Pinkish-gr (10YR6/2)	Sand

[1] br = brown, gr = gray, dk = dark.
[2] By field estimation expressed as USDA particle size class.

more friable than the underlying bentonite into which it grades. The nearly white color allows easy distinction between the tonstein, the overlying dark reddish brown lignitic or carbonaceous strata, and the underlying, yellow to pale yellow, more compact bentonite. The upper portion of the tonstein bed at site 2 shows an indistinct layering or lamination. At all three sites, the kaolinized, pale colored tonstein grades downwards into the underlying bentonite. The transition is gradual and occurs over a distance of about 1–4 mm.

As a result of exposure to weathering, sulfide minerals (e.g., pyrite) in these strata have oxidized to produce sulfuric acid. The relatively low pH (Table 1) suggests that recent weathering has particularly affected sites 2 and 3 where the volcanic layer is much closer to the surface (Figure 2) than at site 1. Both gypsum and jarosite are prominent at sites 2 and 3.

MINERALOGY AND PETROLOGY

Bentonite

Smectite is the dominant mineral in the bentonite (Figure 3b). The smectite shows the characteristic leafy or flaky morphology in the SEM (Figure 4c). The XRD data in Figure 5 indicate that a small amount of kaolinite (indicated by the 7.2-Å peak) is also present in the fine (<0.2 μm) clay fraction from the bentonite. This observation is supported by the IR data (Figure 6) which are more sensitive for detecting small amounts of kaolinite in the presence of larger amounts of smectite. Kaolinite is indicated by the 3695-cm^{-1} bands due to absorption of inner-surface hydroxyls (Farmer, 1974). The 3620-cm^{-1} band is due to stretching of Al_2OH bonds in both kaolinite and smectite (Farmer, 1974). The very broad absorption band in the OH-stretching region (3620–3650 cm^{-1}) is indicative of extensive substitution of Al by Mg and Fe in the octahedral sites of the smectite (Farmer, 1974). Such substitution is also indicated by the OH-bending region (950–800 cm^{-1}) which shows several definite peaks characteristic of the various bonds in the smectite (Figure 6). Based on the IR data, the smectite present in the bentonite is dioctahedral and Al is the major cation in the octahedral sites.

Tonstein

Kaolinite is the most abundant mineral in the tonstein (Figure 3a). The XRD data for the kaolinite in the tonstein are compared in Table 2 with those reported by Berry (1973). The very high resolution of the non-basal kaolinite reflections near 20°2θ (Figure 3a) indicates that the kaolinite is well crystallized and highly ordered (Brindley, 1980). Scanning electron microscopy shows characteristic vermicular growths and books of kaolinite in the tonstein bed (Figure 4). Distinctive

https://doi.org/10.1346/CCMN.1984.0320403 Published online by Cambridge University Press

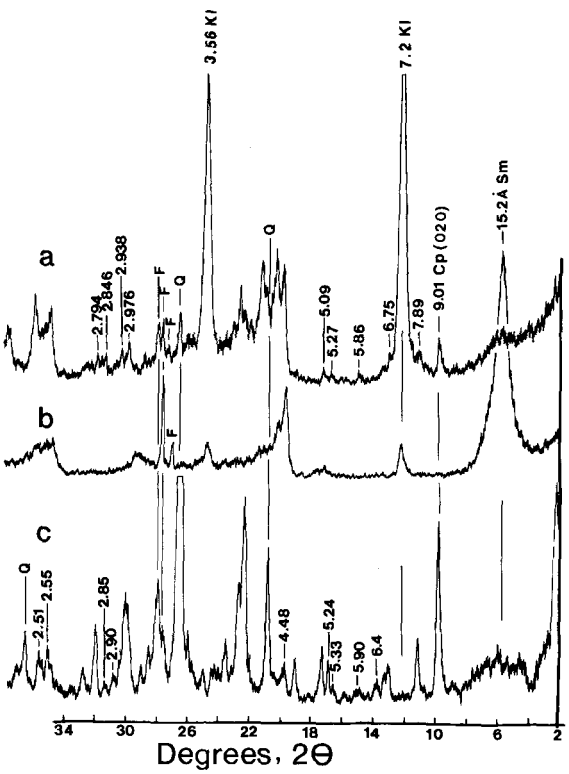

Figure 3. X-ray powder diffraction patterns of bulk samples from (a) tonstein, (b) bentonite, and (c) lignitic bed below the bentonite at site 1. Quartz (Q) and clinoptilolite (Cp) are dominant in the lignitic bed. The tonstein and bentonite layers contain mainly kaolinite (Kl) and smectite (Sm), respectively, as well as minor quartz. All unlabeled peaks of (a) and (c) were assigned to kaolinite and clinoptilolite, respectively (see Table 2).

tabular and vermicular kaolinite was also observed in thin sections (Figure 7). The delicate morphology of the vermicular kaolinite indicates that the kaolinite is not detrital but formed *in situ* (Williamson, 1970; Keller and Hanson, 1975).

Both the tonstein and bentonite strata contain much less quartz than the associated lignitic strata above and below (Figure 3). The quartz grains in the tonstein bed show a distinct angular, elongate morphology (Figure 7a) characteristic of volcanic quartz (Williamson, 1970). The residue remaining after differential dissolution of the kaolinite in the tonstein (by the HF treatment) contained mainly quartz, cristobalite, zircon, and anatase (Figure 8). The zircon was concentrated from the silt fraction of the tonstein bed by heavy liquid techniques. The XRD patterns for the heavy mineral fraction showed distinct peaks of zircon (3.30 Å) and quartz (3.34 Å). Euhedral, silt-size zircon crystals containing fluid or gaseous inclusions were commonly observed in the heavy mineral fraction from the tonstein bed (Figure 7b). Sanidine was identified in the silts from the tonstein by the three-peak method of Wright (1968).

Table 2. X-ray powder diffraction data for kaolinite in tonstein and clinoptilolite in lower lignitic strata (site 1).

Kaolinite					Clinoptilolite				
hkl	JCPDS 12-447	I/I_0	Yegua Fm.[1]	I	*hkl*	JCPDS 22-1236	I/I_0	Yegua Fm.[2]	I
001	7.15	50	7.12	VS	020	8.92	100	9.02	VS
020	4.46	75	4.46	S	002	7.97	4	7.92	S
$1\bar{1}0$	4.34	85	4.34	S	$10\bar{1}$	6.78	2	6.80	M
$11\bar{1}$	4.16	65	4.16	S	031	5.61	2	5.60	W
$1\bar{1}\bar{1}$	4.11	40	4.11	Sh	112	5.15	8	5.12	S
$02\bar{1}$	3.83	50	3.84	W	130	4.65	14	4.64	S
021	3.72	20	—		$10\bar{3}$	4.35	2	—	
002	3.56	50	3.56	VS	132, 004	3.96	55	3.97	VS
111	3.37	12	—		042	3.90	55	3.91	VS
112	3.148	4	—		$14\bar{1}$	3.74	8	3.77	S
022	2.736	4	—		$21\bar{1}$	3.55	6	3.55	M
$20\bar{1}$	2.553	85	2.56	S	$051, 11\bar{4}$	3.48	4	3.42	S
$13\bar{1}$	2.521	50	2.52	Sh	202	3.32	4	3.32	Sh
$13\bar{1}$	2.484	85	2.49	S	$22\bar{2}$	3.17	14	3.17	S
					222	3.12	16	3.12	M
					231	3.07	8	3.07	M
					044	2.974	80	2.97	VS
					$035, 12\bar{5}$	2.793	15	2.794	VS
					$16\bar{1}$	2.728	35	2.72	M
					220	2.419	16	2.42	M

Relative intensity (I): very strong (VS); strong (S); medium (M); weak (W); shoulder (Sh).
[1] Figure 3a.
[2] Figure 3c.

https://doi.org/10.1346/CCMN.1984.0320403 Published online by Cambridge University Press

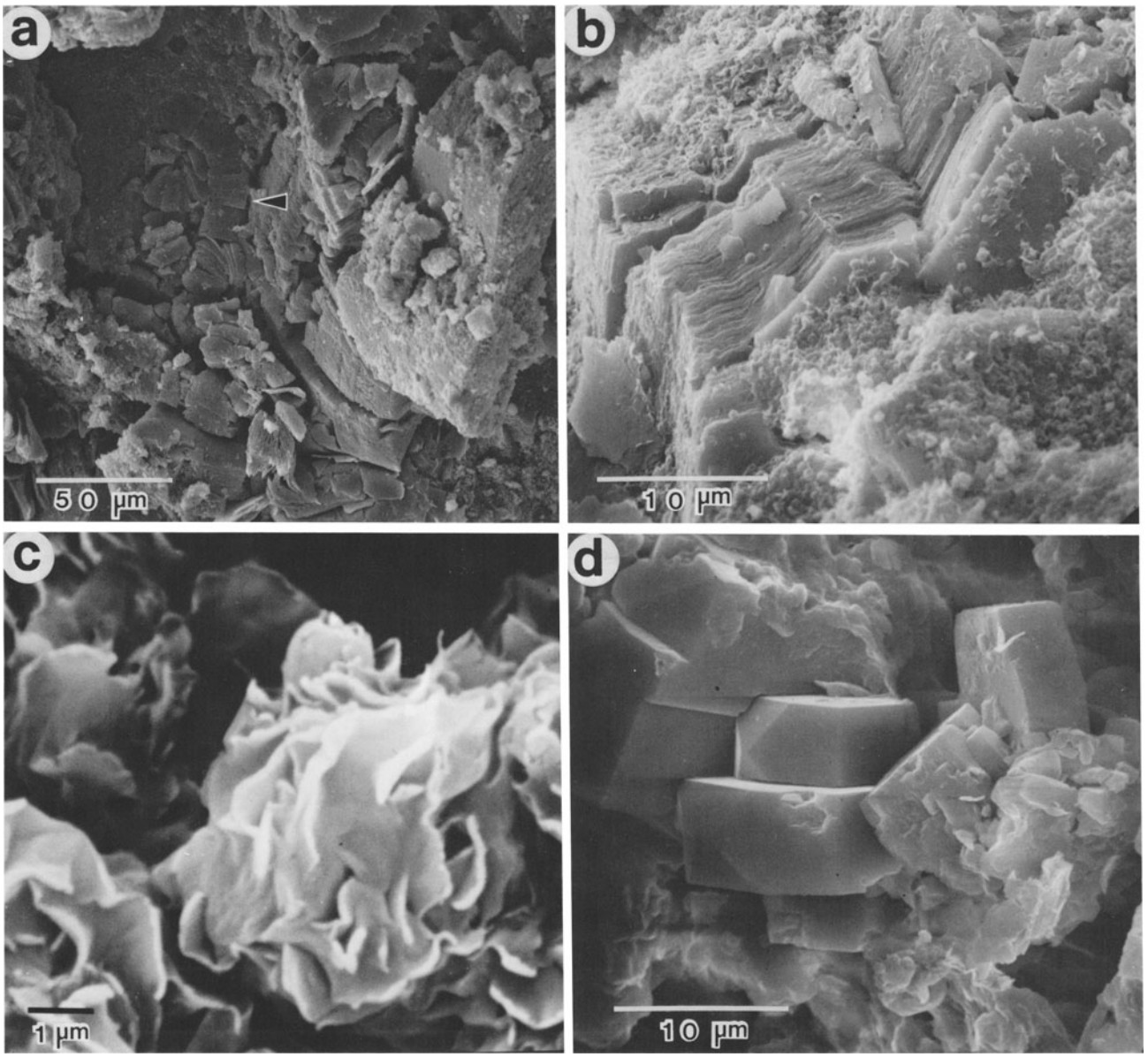

Figure 4. Scanning electron micrographs showing (a) vermicular kaolinite (indicated by arrow), (b) books of kaolinite in tonstein, (c) leafy crystallites of smectite in the bentonite, and (d) clinoptilolite crystals in the underlying lignitic bed. The clinoptilolite crystals show the typical coffin-shape morphology. All samples are from site 1.

Tonstein-bentonite transition

The transitional zone between the tonstein and bentonite varies in thickness from one to several millimeters. TEM and SEM studies revealed the presence of both halloysite and smectite in this zone (Figure 9). The halloysite occurs as isolated groups of spheroidal particles, some of which are closely associated with the leafy crystallites of smectite (Figure 9b). Locally, halloysite spheroids appear to have crystallized on the surface of the smectite flakes, suggesting that the halloysite precipitated at a later stage than the smectite. The occurrence of halloysite is restricted to the transitional zone.

A section across the tonstein-bentonite transition shows that the kaolinization process started in pores and fissures within the bentonite resulting in precipitation of a cryptocrystalline ground mass of 1:1 phyllosilicates (Figure 10a). Larger kaolinite books are more abundant further away from the weathering front. The fully developed vermicular kaolinite contains inclusions of continuous layers of organic matter running along the entire length of the crystal (Figure 10b). In

https://doi.org/10.1346/CCMN.1984.0320403 Published online by Cambridge University Press

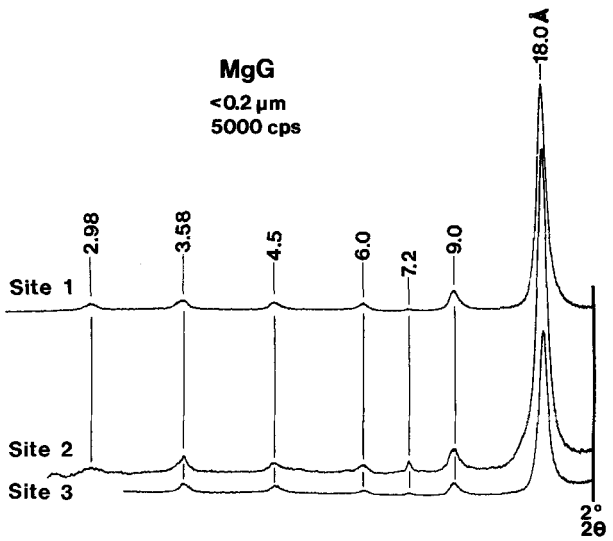

Figure 5. X-ray powder diffraction patterns of the fine clay fractions (<0.2 μm) indicate that smectite (18.0-, 9.0-, 6.0-, 4.5-, and 2.98-Å peaks) is the dominant mineral in the bentonite with minor kaolinite (7.2- and 3.58-Å peaks).

the less-developed kaolinite books, the organic matter forms rims around the edges of the crystals.

Distribution of clinoptilolite

Quartz and clinoptilolite are the most abundant minerals in the lignitic beds above the tonstein and below the bentonite (Figure 3c) at all three sites. Also, a small amount of clinoptilolite is in the tonstein (Figure 3a) at all three sites. The clinoptilolite crystals show the characteristic "coffin-shape" morphology (Figure 4d) of the mineral (Mumpton and Ormsby, 1976). The XRD data for the clinoptilolite in these strata are compared in Table 2 with those reported by Berry (1973). The 020 reflection of the clinoptilolite at 9.02 Å was not affected by heating overnight at 450°C, as is characteristic of a Na- and K-rich clinoptilolite (Brown, 1980). Clinoptilolite is most abundant in the lignitic bed immediately below the bentonite and gradually decreases with increasing depth. A photograph of the various strata discussed and their bulk mineralogy are shown in Figure 11.

Chemical composition

The smectitic bentonite contains much higher concentrations of Fe and Mg than the kaolinitic tonstein (Table 3). In contrast, Ti, Ba, and, to some extent, Al are consistently more abundant in the tonstein than they are in the bentonite. The least kaolinitic bentonite at site 1 shows the highest Na content (Table 3). The tonstein stratum at all three sites contains more Na and K than the corresponding bentonite, owing partly to the presence of Na- and K-rich clinoptilolite in the

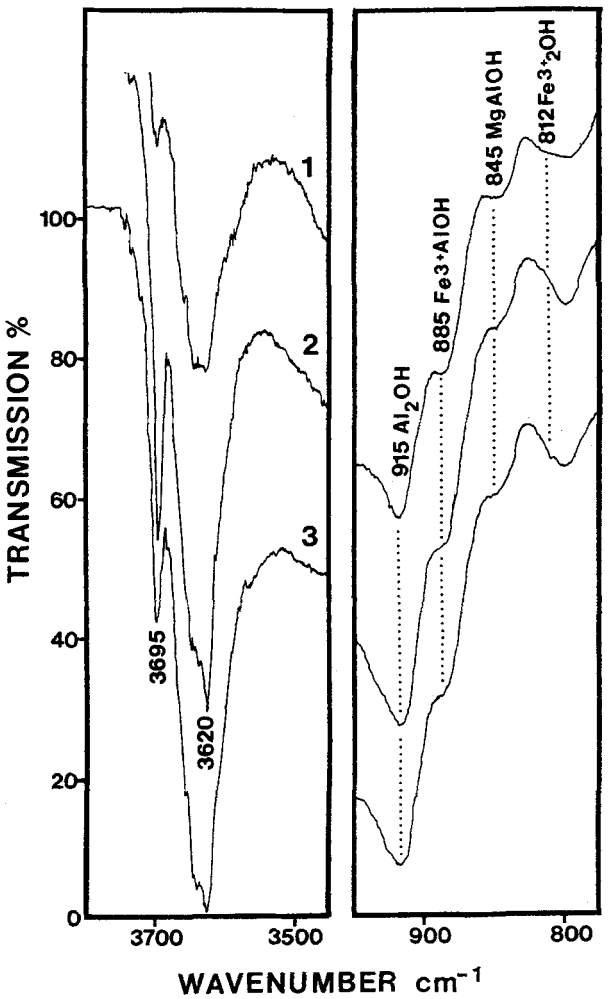

Figure 6. Infrared spectra of the fine (<0.2 μm) clay samples from bentonite at sites 1, 2, and 3. The spectra indicate the presence of a dioctahedral smectite with extensive substitution of Al by Fe and Mg in the octahedral sites.

tonstein. The greater quantities of Ca in the bentonite compared to the tonstein indicate that the dominant exchangeable cation in the smectite is Ca.

GENETIC INTERPRETATION

Evidence for volcanic origin

The presence of cristobalite, sanidine, and zircon crystals with gaseous or liquid inclusions and the morphology and much lower quartz content in the tonstein and bentonite strata compared to the overlying and underlying strata all suggest a volcanic origin of the tonstein and bentonite. From the stratigraphic section in Figure 2, it is apparent that the tonstein and bentonite strata at all three sites are part of a single deposit of volcanic ash. The consistent pattern of TiO_2/ZrO_2, BaO/TiO_2, TiO_2/Al_2O_3, and TiO_2/SrO ratios of the

https://doi.org/10.1346/CCMN.1984.0320403 Published online by Cambridge University Press

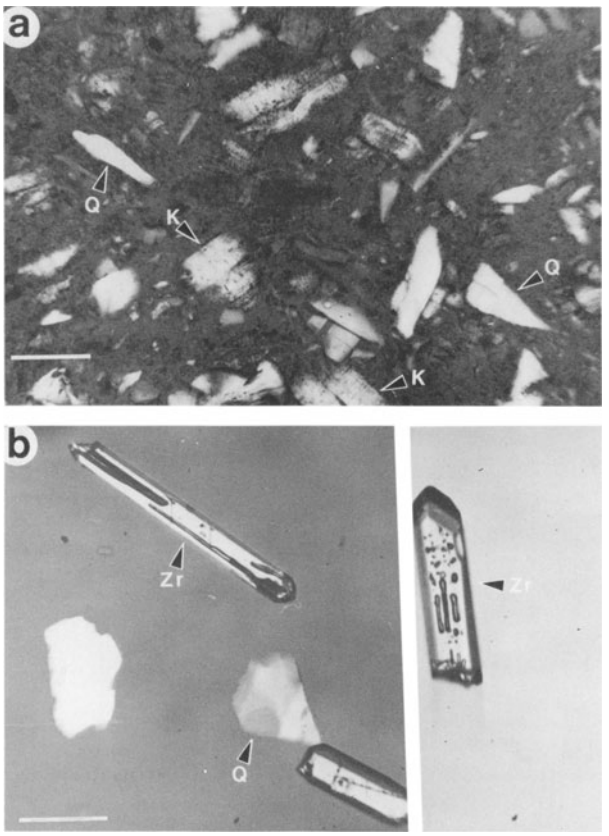

Figure 7. Photomicrographs showing: (a) morphology of kaolinite and quartz; and (b) zircon crystals in the tonstein layer at site 1. Angular, elongate grains of quartz (Q), books of kaolinite (K), and euhedral crystals of zircon (Zr) containing liquid or gaseous inclusions are characteristic of the tonstein.

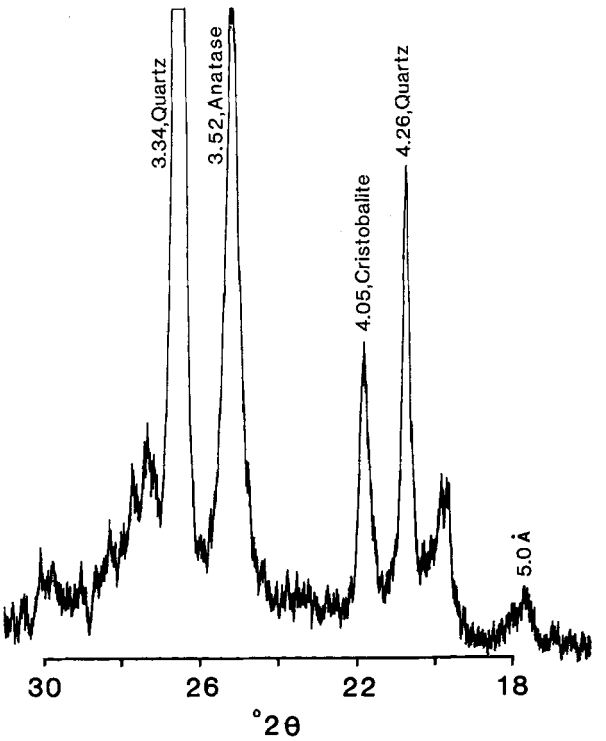

Figure 8. X-ray powder diffraction pattern of the residue obtained by differentially dissolving kaolinite from the tonstein bed at site 2. Cristobalite (4.05 Å), anatase (3.52 Å), and quartz (4.26 and 3.34 Å) were concentrated in the residue.

bentonite layers at the three sites (Figure 12) suggest that all of these strata developed from volcanic ash of similar composition. Ratios of TiO_2/Al_2O_3 have been used to characterize the parent volcanic ash of British and European tonsteins (Spears and Kanaris-Sotiriou, 1979). High TiO_2/Al_2O_3 ratios (>0.08) are indicative of tonsteins derived from basic volcanic ash, whereas low ratios (<0.02) are characteristic of tonsteins derived from acid volcanic ash. Intermediate values indicate an intermediate composition of the ash or contamination by nonvolcanic materials (usually indicated by presence of abundant detrital quartz). The generally low TiO_2/Al_2O_3 ratios (<0.02) for the bentonite bed at all three sites suggest that the original ash was probably acid.

The TiO_2/Al_2O_3 ratios of the tonstein bed, however, are greater than those of the associated bentonite at all the three sites. Moreover, the TiO_2/Al_2O_3 and BaO/TiO_2 ratios of the tonstein gradually increase, whereas the TiO_2/ZrO_2 ratios decrease from site 1 to site 3 (Figure 12). These variations may be related to the intensity of weathering or contamination by nonvolcanic materials. The accumulation of Ba in tonsteins has been ascribed to formation of minerals of the plumbogummite series (hydrated alumino-phosphates of Ba, Sr, and Ca) during weathering (Price and Duff, 1969). These minerals, however, were not detected in the tonstein investigated in the present study, although greater concentrations of Ba were found in the tonstein compared to the bentonite (Figure 12).

The tonstein and bentonite strata are much thinner and laterally discontinuous at site 1 which suggests that some of the volcanic materials were, perhaps, eroded from this site before burial. The indistinct bedding of the upper portion of the tonstein strata at site 2 also suggests that there was some mixing of the volcanic and nonvolcanic materials after deposition in the swamp. Tonsteins developed from such admixed materials are classified as strato-tonsteins (Williamson, 1970). The upper portion of the tonstein at site 2 can be classified as a strato-tonstein because it contains much more detrital quartz (based on XRD) than the lower portion (ortho-tonstein) which is developed entirely from volcanic materials (Figure 11). The lateral uniformity in thickness of the tonstein and bentonite

https://doi.org/10.1346/CCMN.1984.0320403 Published online by Cambridge University Press

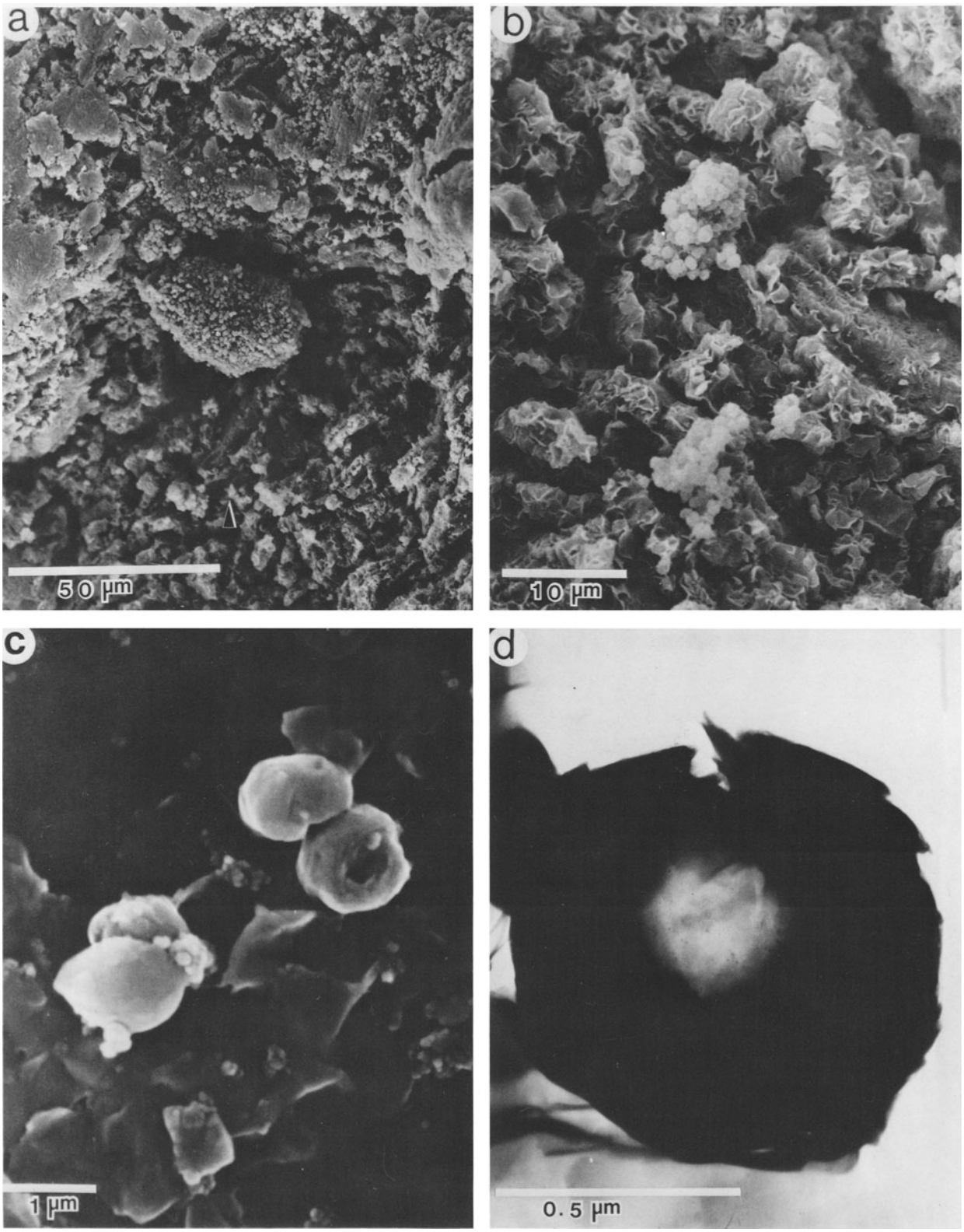

Figure 9. Scanning (SEM) and transmission (TEM) electron micrographs showing halloysite and smectite in the transition zone between tonstein and bentonite: (a) SEM showing the transition from altered bentonite containing halloysite (top) to

https://doi.org/10.1346/CCMN.1984.0320403 Published online by Cambridge University Press

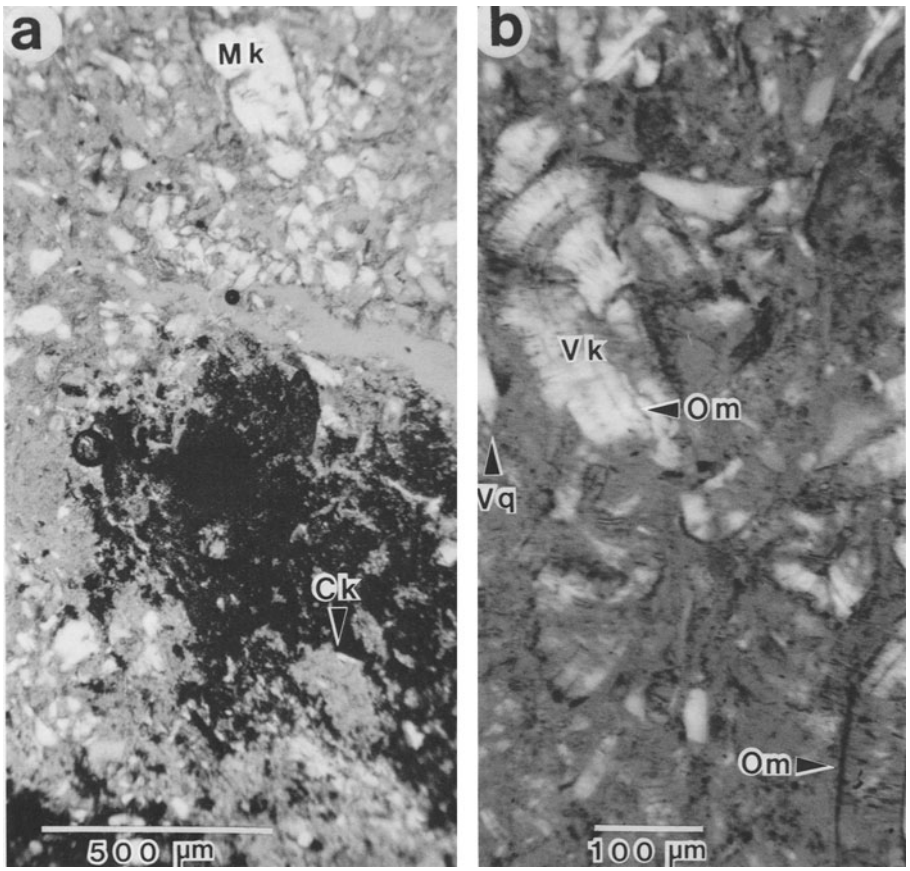

Figure 10. Photomicrographs of a thin section (a) cut across the boundary between the tonstein (top) and bentonite (bottom). Cryptocrystalline groundmass (Ck) of 1:1 phyllosilicates (kaolinite and halloysite) precipitated first in the pores and fissures. Large books of kaolinite (Mk) are more abundant further away from the weathering front. (b) Fully developed vermicular kaolinite (Vk) in the tonstein contain organic matter (Om) layers. Grains of volcanic quartz (Vq) are small and angular. (Crossed polars).

strata at site 3 indicates that there was minimal disturbance of the ash after deposition in the Eocene swamp.

Weathering sequence

The sequence of the major diagenetic events and processes following the deposition of the volcanic ash in the swamp (phase 1) are illustrated in Figure 13. The moist environment in the swamp favored crystallization of smectite (phase 2) rather than clinoptilolite. According to Grim and Güven (1978), crystallization of either smectite or clinoptilolite can occur following deposition of volcanic materials in swamps. Whether the ash is altered to smectite or zeolite (clinoptilolite) depends on the activities of H^+, alkali and alkaline earth cations, H_4SiO_4, and $Al(OH)_4^-$ (Hay, 1978). The formation of smectite in the bentonite layer (phase 2) was probably favored by high activities of Mg, whereas abundant H_4SiO_4, Na, and K favored precipitation of clinoptilolite in the underlying lignitic strata. Precipitation of the clinoptilolite probably occurred as solutions from the bentonite layer above percolated through the lignitic stratum below. Leaching of K and Na from the ash seemingly precluded the formation of clinoptilolite in the bentonite during phase 2. Pevear *et al.* (1980) observed that the presence or absence of clinoptilolite in the bentonites they investigated was related to the degree of leaching following

←

less altered bentonite below; (b) a close-up view of the lower section of (a) (indicated by arrow) showing an association of halloysite and leafy crystallites of smectite; (c) and (d) SEM and TEM, respectively, showing the spheroidal morphology of individual halloysite particles. Specimen from site 1.

https://doi.org/10.1346/CCMN.1984.0320403 Published online by Cambridge University Press

Table 3. Chemical composition (%) of bulk samples from the tonstein and bentonite beds.

	Site 1		Site 2			Site 3	
	T[1]	B[2]	S-T[3]	O-T[4]	B	T	B
SiO_2	48.67	52.62	56.59	52.22	53.53	50.02	58.19
Al_2O_3	29.47	24.55	24.53	28.76	25.79	28.29	20.33
Fe_2O_3	0.65	4.27	0.99	1.37	3.02	0.38	3.12
TiO_2	0.383	0.190	0.573	0.366	0.206	0.550	0.192
K_2O	0.98	0.21	1.33	1.14	0.16	1.38	0.24
Na_2O	1.03	0.78	0.91	0.80	0.18	0.91	0.29
ZrO_2	0.004	0.002	0.006	0.002	0.002	0.012	0.002
BaO	0.061	0.017	0.127	0.085	0.016	0.180	0.034
MgO	0.35	1.39	0.51	0.35	1.29	0.41	1.28
CaO	0.86	1.39	1.01	0.77	1.311	1.06	1.44
SrO	0.037	0.023	0.072	0.036	0.020	0.102	0.021
Cr_2O_3	0.007	0.008	0.009	0.006	0.007	0.009	0.009
MnO_2	0.008	0.007	0.009	0.007	0.009	0.096	0.105
L.O.I[5]	12.3	10.05	11.15	11.70	10.99	11.80	12.78
C[6]	0.61	0.32	1.87	0.92	0.90	0.22	0.58
Total	95.24	95.82	99.67	98.49	97.36	95.42	98.56

[1] Tonstein.
[2] Bentonite.
[3] Strato-tonstein.
[4] Ortho-tonstein.
[5] Loss on ignition from 110° to 950°C.
[6] Total C.

deposition of the ash in swamps. The bentonites least exposed to leaching contained clinoptilolite, whereas the most leached bentonites contained smectite and minor quantities of kaolinite.

After deposition of the ash, swamp vegetation was reestablished (phase 3). The accumulation of organic matter, which had been interrupted during deposition of ash, commenced again. Dissolution of the smectite and recrystallization of 1:1 phyllosilicates (kaolinite and halloysite) occurred as humic solutions moved downward through the bentonite layer. The kaolinization process started in pores and fissures within the bentonite where halloysite was initially precipitated. On further weathering, the groundmass containing cryptocrystalline forms of kaolin was gradually reorganized through a series of dissolution and reprecipitation cycles into large books of kaolinite surrounded by rims of organic matter (Figure 10b).

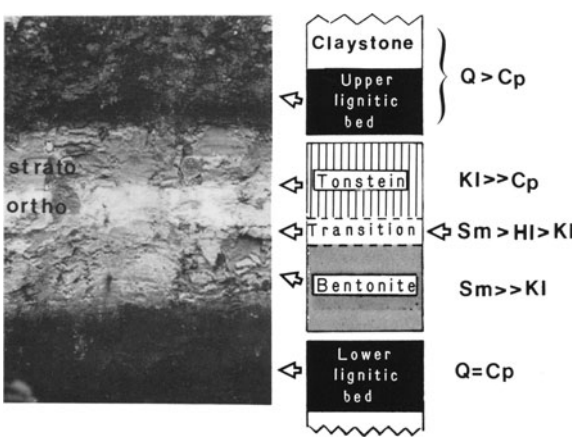

Figure 11. Generalized lithologic column showing relative mineralogical compositions of bentonite, tonstein, and lignitic strata (photograph on the left): Kl = kaolinite; Sm = smectite; Q = quartz; Cp = clinoptilolite; Hl = halloysite.

Formation of vermicular kaolinite

The formation of large vermicular aggregates of kaolinite in the tonstein followed the stages of development described by Moore (1964). The early stages are represented by a minimum orientation of the organic matter around the kaolinite crystallites. In the large crystals, the organic matter forms either rims around the edges of the kaolinite crystals or continuous layers, running along the entire length of the particle. The presence of organic matter inclusions within the kaolinite particle suggests that crystallization of kaolinite occurred intermittently. Periods of crystal growth were interrupted by deposition of organic matter layers on the surfaces of newly formed crystals.

Although it is generally accepted that tonsteins are *in situ* alteration products of volcanic ash beds, the fact that kaolinite, which is the dominant mineral in these strata, occurs in a variety of forms has not been adequately explained. Vermicular aggregates of kaolinite with sizes of up to several millimeters are known in tonsteins and were once known as leverrierite (Millot, 1970). In fact, the most widely accepted classification of tonsteins is based on micromorphological features of the kaolinite (Williamson, 1970). The results obtained in the present study indicate a genetic progres-

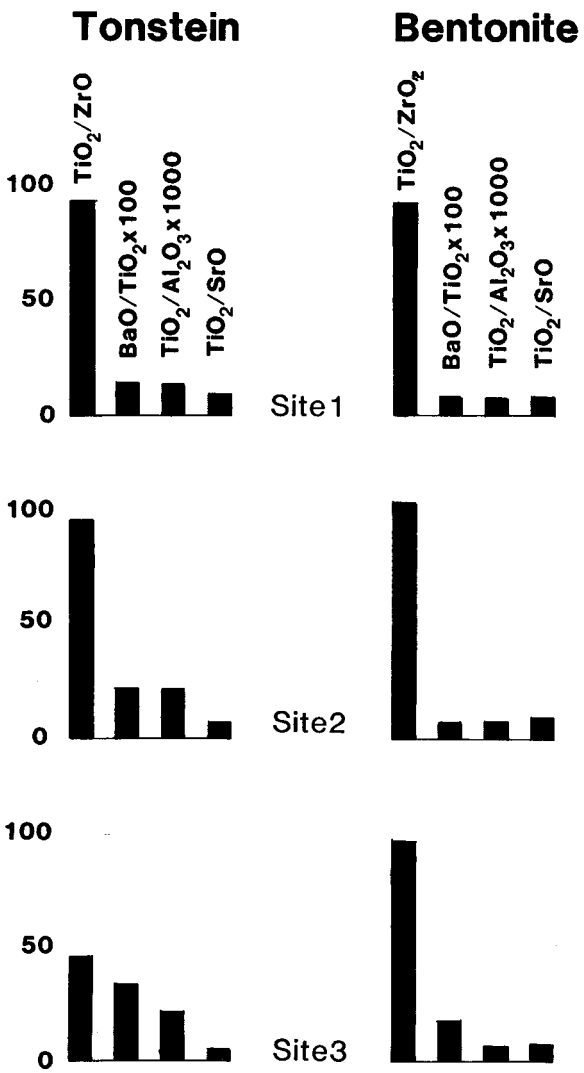

Figure 12. Relative abundancies of Ti, Zr, Sr, Ba, and Al in the tonstein and bentonite layers exposed at sites 1, 2, and 3.

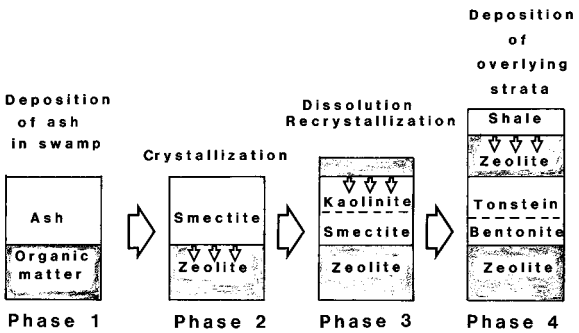

Figure 13. Summary of the proposed major processes affecting the volcanic ash following deposition in the swamp: Zeolite = clinoptilolite.

sion from the cryptocrystalline forms to the large books of kaolinite in tonsteins and that kaolinization takes place in at least two stages. In the first stage, rapid crystallization occurred and resulted in the formation of cryptocrystalline halloysite and kaolinite along the weathering front. The second stage was more gradual and probably involved dissolution of the cryptocrystalline halloysite and kaolinite and formation of large books of kaolinite. These conclusions accord with the work of Morgan *et al.* (1979) who investigated morphological characteristics of kaolinite in a smectitic volcanic bed and showed an increasing degree of kaolinization from bottom to top. These investigators concluded that dissolution/recrystallization cycles played a major role and resulted in the formation of large books and vermiforms of kaolinite in the most completely kaolinized portions at the top of the bed. The kaolinite crystals in the least kaolinized parts of the bed were much smaller.

Halloysite and clinoptilolite in the tonstein bed

The presence of halloysite in altered volcanic materials and soils derived from them has been widely reported (Kirkman, 1981; Saigusa *et al.*, 1978; Askenasy *et al.*, 1973; Dixon and McKee, 1974). Very little, however, has been written about the occurrence of this mineral in tonsteins. The particular conditions favoring the formation of halloysite along the boundary between the tonstein and bentonite are not clearly understood. Saigusa *et al.* (1978) found that halloysite formed where silica, leached from overlying volcanic strata, was added to buried organic layers. They concluded that reaction of the silica with the Al, that was, perhaps, complexed by the organic matter, resulted in the formation of halloysite. It is possible that a similar mechanism operated during alteration of the bentonite to tonstein. Here, however, downward translocation of the Al, complexed by humic solutions, might have triggered the precipitation of halloysite along the weathering front. Confinement of the halloysite to the transition from tonstein to bentonite suggests that the formation of the halloysite preceded deposition of the overlying strata (phase 4 in Figure 13).

After deposition of the overlying strata, redistribution of silica-rich solutions resulted in the precipitation of clinoptilolite in the tonstein and in the nonvolcanic strata above the tonstein. Low permeability or some other factors may have inhibited continued downward movement of these solutions and, hence, precipitation of clinoptilolite in the bentonite strata at this stage.

SUMMARY AND CONCLUSIONS

Volcanic ash deposited in a late Eocene swamp was initially altered to smectite. Leaching of Na, K, and silica from the volcanic ash resulted in concentration

https://doi.org/10.1346/CCMN.1984.0320403 Published online by Cambridge University Press

of these ions in the underlying nonvolcanic strata, thus favoring precipitation of clinoptilolite in the lignitic and nonlignitic strata below the bentonite. Subsequent weathering and leaching resulted in the dissolution of smectite and precipitation of halloysite and kaolinite as tonstein formed in the upper parts of the bentonite bed. Halloysite is restricted to the transitional interval between the kaolinitic tonstein and the remaining smectitic bentonite, suggesting that the halloysite formed first as the smectite-rich bentonite gradually altered to the kaolinite-rich tonstein.

The formation of the tonstein is believed to be the product of processes that preceded deposition of the immediately overlying strata as indicated by the crystallization of clinoptilolite on edges of kaolinite crystallites. Present-day weathering produced the low pH values of those sites that are nearest to the modern land surface (sites 2 and 3, figure 2). The presence of gypsum and jarosite at these two sites implies that pyrite oxidation and acid sulfate weathering may also have influenced the weathering of the bentonite at these two sites. The data available do not permit conclusive statements on how much the modern weathering environment enhanced kaolinization of the bentonite bed.

ACKNOWLEDGMENTS

This research was supported by the Center for Energy and Mineral Resources, Texas A&M University. We thank Mr. R. A. Stockton for his help in analyzing the samples by the inductively coupled plasma emission spectroscopy, and Mr. J. R. Scott for help with electron microscopy work. Drs. D. R. Pevear, P. C. Franks, and B. F. Bohor provided valuable comments and suggestions.

REFERENCES

Askenasy, P. E., Dixon, J. B., and McKee, T. R. (1973) Spheroidal halloysite in a Guatemalan soil: *Soil Sci. Soc. Amer. Proc.* **37,** 799–803.

Berg, R. R. (1970) Stratigraphy of the Claiborne Group: in *Claiborne Outcrops in the Brazos Valley, Southwest Texas,* R. R. Berg, ed., *Geol. Soc. Amer., South-cent. Sect., Field Trip Guidebook,* 13–16.

Bernas, B. (1968) A new method for decomposition and comprehensive analysis of silicates by atomic absorption spectrometry: *Anal. Chem.* **40,** 1682–1686.

Berry, L. G. (1973) *Powder Diffraction File for Minerals:* Joint Committee on Powder Diffraction Standards, Swarthmore, Pennsylvania, 833 pp.

Brindley, G. W. (1980) Order-disorder in clay mineral structures: in *Crystal Structures of Clay Minerals and their X-ray Identification,* G. W. Brindley and G. Brown, eds., Mineralogical Society, London, 125–195.

Brown, G. (1980) Associated minerals: in *Crystal Structures of Clay Minerals and their X-ray Identification,* G. W. Brindley and G. Brown, eds., Mineralogical Society, London, 361–410.

Carr, C. E. (1973) Gravimetric determination of soil carbon using the LECO induction furnace. *J. Sci. Food Agric.* **24,** 1091–1095.

Dixon, J. B. and McKee, T. R. (1974) Internal and external morphology of tubular and spheroidal halloysite particles: *Clays & Clay Minerals* **22,** 127–137.

Farmer, V. C. (1974) The layer silicates: in *The Infrared Spectra of Minerals,* V. C. Farmer, ed., Mineralogical Society, London, 331–363.

Grim, R. E. and Güven, N. (1978) *Bentonites:* Elsevier, Amsterdam, 126–137.

Hay, R. L. (1978) Geologic occurrence of zeolites: in *Natural Zeolites: Occurrence, Properties and Use,* L. B. Sand and F. A. Mumpton, eds., Pergamon Press, Elmsford, New York, 135–145.

Innes, R. P. and Pluth, D. J. (1970) Thin section preparation for petrographic and microprobe analysis: *Soil Sci. Soc. Amer. Proc.* **34,** 484–485.

Jackson, M. L. (1974) *Soil Chemical Analysis—Advanced Course:* 2nd ed., published by the author, Madison, Wisconsin, 895 pp.

Kaiser, W. R. (1974) Texas lignite: near-surface and deep-basin resources: *Texas Bur. Econ. Geol. Rept. Invest.* **79,** 70 pp.

Keller, W. D. and Hanson, R. F. (1975) Dissimilar fabrics by scan electron microscopy of sedimentary versus hydrothermal kaolins in Mexico: *Clays & Clay Minerals* **23,** 201–204.

Kirkman, J. H. (1981) Morphology and structure of halloysite in New Zealand tephras: *Clays & Clay Minerals* **29,** 1–9.

Loughnan, F. C. (1978) Flint clays, tonsteins and the kaolinite clay rock facies: *Clay Miner.* **13,** 387–400.

Mathews, A. L. (1950) Geology of Brazos County, Texas: *Texas A&M College, Eng. Exp. Station, Res. Rept.* **14,** 14 pp.

Millot, G. (1970) *Geology of Clays:* Springer-Verlag, New York, 419 pp.

Moore, L. R. (1964) The *in situ* formation and development of some kaolinite macrocrystals: *Clay Miner. Bull.* **5,** 338–352.

Morgan, D. J., Highley, D. E., and Bland, D. J. (1979) A montmorillonite, kaolinite association in the Lower Cretaceous southeast England: in *Proc. Int. Clay Conf., Oxford, 1979,* M. M. Mortland and V. C. Farmer, eds., Elsevier, Amsterdam, 301–310.

Mumpton, F. A. and Ormsby, W. C. (1976) Morphology of zeolites in sedimentary rocks by scanning electron microscopy: *Clays & Clay Minerals* **24,** 1–23.

Norrish, K. (1968) Some phosphate minerals of soils: *Trans. 9th Int. Congr. Soil Sci., Adelaide, Australia* **II,** 713–723.

Pevear, D. R., Williams, V. E., and Mustoe, G. E. (1980) Kaolinite, smectite and K-rectorite in bentonites: relation to coal rank at Tulameen, British Columbia: *Clays & Clay Minerals* **28,** 241–254.

Price, N. B. and Duff, P. M. D. (1969) Mineralogy and chemistry of tonsteins from carboniferous sequences in Great Britain: *Sedimentology* **13,** 45–69.

Roberson, H. E. (1964) Petrology of Tertiary bentonites of Texas: *J. Sediment. Petrol.* **34,** 401–411.

Saigusa, M., Shogi, S., and Kato, T. (1978) Origin and nature of halloysite in ando soils from Towada tephra, Japan: *Geoderma* **20,** 115–129.

Spears, D. A. and Kanaris-Sotiriou, R. (1979) A geochemical and mineralogical investigation of some British and other European tonstein: *Sedimentology* **26,** 407–425.

Williamson, I. A. (1970) Tonsteins—their nature, origins and uses: *Mining Mag.* **122,** 119–125, 203–211.

Wright, T. L. (1968) X-ray and optical study of alkali feldspar, Pt. 2: *Amer. Mineral.* **53,** 88–104.

Zhou, Y., Ren, Y., and Bohor, B. F. (1982) Origin and distribution of tonsteins in Late Permian Coal seams of southwestern China. *Int. J. Coal Geol.* **2,** 49–77.

(Received 25 August 1982; accepted 9 March 1984)

Резюме—Пласт, обогащенный каолинитом (тонштейн) и ассоциированный бентонит в верхней части формации Егуа в Коледж Стейшин в восточно-центральном Техасе, формировались путем виутрипластовых процессов эрозии в болоте позднего эоцена. Рентгеновская порошковая дифракция, инфракрасная спектроскопия, петрографические исследования, а также сканнинговая и трансмисионная микроскопия указывали не только на то, что диоктаэдрический смектит и грубо кристаллический каолинит являются главными минералами в бентоните и тонштейне, соответственно, но что криптокристаллический галлуазит и каолинит расположены вдоль фронта эрозии (переходная зона) между тонштейном и бентонитом. Когда эрозия прогрессировала, криптокристаллические минералы постепенно рекристаллизировались, чтобы производить грубые книгоподобные и червеобразные росты каолинита, характеристические для тонштейна. Небольшие количества кристобалита, санидина и идиоморфных кристаллов циркона с жидкими или газовыми включениями согласовывались с формированием бентонита путем изменения вулканического пепела. Клиноптилолит в слое бурого угля и песчаника ниже бентонита формировался, вероятно, из ионов, которые выделялись во премя видоизменения вулканических материалов в смектит, но клиноптилолит в тонштейне и перекрывающих породах, вероятно, образовывался после каолинизации бентонита. [E.G.]

Resümee—Eine Kaolinit-reiche Lage (Tonstein) und ein damit zusammenhängender Bentonit im oberen Teil der Yegua Formation bei College Station, Ostzentraltexas, wurden durch *in situ* Verwitterungsprozesse in einem späteozänen Moor gebildet. Röntgenpulverdiffraktometrische, infrarotspektroskopische und petrographische sowie raster- und transmissionselektronenmikroskopische Untersuchungen zeigten nicht nur, daß dioktaedrischer Smektit und grobkristallisierter Kaolinit die vorherrschenden Minerale in dem Bentonit bzw. in dem Tonstein sind, sondern daß auch kryptokristalliner Halloysit und Kaolinit entlang der Verwitterungsfront (Übergangszone) swischen Tonstein und Bentonit auftreten. Wenn die Verwitterung fortgeschritten ist, rekristallisierten die kryptokristallinen Minerale allmählich und führten zu dem groben bücherförmigen und wurmähnlichen Wachstum von Kaolinit, das für den Tonstein charakteristisch ist.

Geringe Gehalte an Cristobalit, Sanidin, und idiomorphen Zirkonkristallen mit flüssigen oder gasförmigen Einschlüssen stimmen mit der Bildung des Bentonites durch Umwandlung von vulkanischer Asche überein. Klinoptilolit in den Lignitlagen und im Sandstein unter dem Bentonit wurde wahrscheinlich aus Ionen gebildet, die während der Umwandlung des vulkanischen Materials zu Smektit freigesetzt wurden. Der Klinoptilolit in dem Tonstein und den darüberliegenden Schichten scheint nach der Kaolinisierung des Bentonites gebildet worden zu sein. [U.W.]

Résumé—Un lit riche en kaolinite (tonstein) et une bentonite associée dans la partie supérieure de la Formation Yegua à College Station, centre-est du Texas, ont été formés par un procédé d'altération *in situ* dans un marais du Bas Eocène. La diffraction aux rayons-X, la spectroscopie infrarouge, des études petrographiques, et la microscopie électronique et à transmission d'électrons montrent non seulement que la smectite dioctaèdrale et la kaolinite grossièrement cristallisée sont les minéraux dominants dans la bentonite et la tonstein respectivement, mais que l'halloysite cryptocristalline et la kaolinite sont localisées le long du front d'altération (zone de transition) entre la tonstein et la bentonite. Au fur et à mesure de la progression de l'altération, les minéraux cryptocristallins se sont graduellement recristallisés pour donner les livres grossiers et les croissances vermiculaires caractéristiques de la tonstein.

De petites quantités de cristobalite, de sanidine, et de cristaux euhédraux de zircon avec des inclusions liquides ou gazeuses s'accordent avec la formation de la bentonite par altération de la cendre volcanique. La clinoptilite dans la couche lignitique et dans le grès en dessous de la bentonite s'est probablement formée à partir d'ions qui avaient été relâchés pendant l'altération de matériaux volcaniques en smectite, mais la clinoptilolite dans la tonstein et les strates susjacentes semble avoir été formée après la kaolinisation de la bentonite. [D.J.]